UNIVERSITY OF WEST LONDON
The Career University

UWL REPOSITORY

repository.uwl.ac.uk

Cooperative SWIPT MIMO-NOMA for reliable THz 6G communications

Oleiwi, Haider W., Saeed, Nagham ORCID logoORCID: https://orcid.org/0000-0002-5124-7973 and Al-Raweshidy, Hamed (2022) Cooperative SWIPT MIMO-NOMA for reliable THz 6G communications. Network, 2 (2). pp. 257-269.

http://dx.doi.org/10.3390/network2020017

This is the Published Version of the final output.

UWL repository link: https://repository.uwl.ac.uk/id/eprint/9003/

Alternative formats: If you require this document in an alternative format, please contact: open.research@uwl.ac.uk

Copyright: Creative Commons: Attribution 4.0

Copyright and moral rights for the publications made accessible in the public portal are retained by the authors and/or other copyright owners and it is a condition of accessing publications that users recognise and abide by the legal requirements associated with these rights.

Take down policy: If you believe that this document breaches copyright, please contact us at open.research@uwl.ac.uk providing details, and we will remove access to the work immediately and investigate your claim.

network

MDPI

Article

Cooperative SWIPT MIMO-NOMA for Reliable THz 6G Communications

Haider W. Oleiwi [1,*], Nagham Saeed [2] and Hamed Al-Raweshidy [1]

[1] Department of Electronic and Electrical Engineering, Brunel University London, London UB8 3PH, UK; hamed.al-raweshidy@brunel.ac.uk
[2] School of Computing and Engineering, University of West London, London W5 5RF, UK; nagham.saeed@uwl.ac.uk
* Correspondence: haider.al-lami@brunel.ac.uk

Abstract: In this paper, cooperative simultaneous wireless information and power transfer (SWIPT) terahertz (THz) multiple-input multiple-output (MIMO) nonorthogonal multiple access (NOMA) are considered. The aim is to improve wireless connectivity, resource management, scalability, and user fairness, as well as to enhance the overall performance of wireless communications and reliability. We optimized the current wireless communication systems by utilizing MIMO-NOMA technology and THz frequencies, exploring the performance and gains obtained. Hence, we developed a path-selection mechanism for the far user to enhance the system performance. The EH SWIPT approach used to improve THz communications performance was investigated. Moreover, we proposed a reliable transmission mechanism with a non-LoS (NLoS) line of THz communications for open areas or any location where the intelligent reflecting surface (IRS) cannot be deployed, in addition to using the cheap decode-forward (DF) relaying instead of IRS. The performance and scalability of the upgradeable system were examined, using adjustable parameters and the simplest modulation scheme. The system presents a noticeable improvement in energy efficiency (EE) and spectral efficiency (SE), in addition to reliability. Accordingly, the outcome showed an improvement in the overall reliability, SE, EE, and outage probability as compared to the conventional cooperative networks of the recent related work (e.g., cooperative MIMO-NOMA with THz) by multiple times with a simpler design, whereas it outperformed our previous work, i.e., cooperative SWIPT SISO-NOMA with THz, by more than 50%, with a doubled individual user gain. This system reduces the transceiver hardware and improves reliability with increasing transmission rates.

Keywords: cooperative networks; energy efficiency; energy harvesting; MIMO-NOMA path selection; outage probability; reliable THz communications; resource management; spectral efficiency

check for updates

Citation: Oleiwi, H.W.; Saeed, N.; Al-Raweshidy, H. Cooperative SWIPT MIMO-NOMA for Reliable THz 6G Communications. *Network* **2022**, 2, 257–269. https://doi.org/10.3390/network2020017

Academic Editor: Christos Bouras

Received: 12 March 2022
Accepted: 22 April 2022
Published: 24 April 2022

Publisher's Note: MDPI stays neutral with regard to jurisdictional claims in published maps and institutional affiliations.

Copyright: © 2022 by the authors. Licensee MDPI, Basel, Switzerland. This article is an open access article distributed under the terms and conditions of the Creative Commons Attribution (CC BY) license (https://creativecommons.org/licenses/by/4.0/).

1. Introduction

The wireless communication field has witnessed a rapid rise with a significant expansion of smart gadgets, new technologies, and modern applications. The critical requirement for fast data transport combined with the global ubiquity of services has resulted in groundbreaking research. Energy efficiency (EE) and spectral efficiency (SE) are two distinct metrics that assess system performance [1–4]. It is critically required to enhance EE and SE to fulfill the strict requirements of diverse emerging applications, adapting to the upgrades of the next era and eliminating power consumption of the required equipment [5–10]. The efficient use of energy has become an inevitable demand in the next generation of 6G to support its practicability and satisfy its needs [11]. Terahertz (THz) communication [12] will have a significant impact on future generations. According to Shannon's equation, SE is determined on the basis of bandwidth (BW) availability. THz represents the unexplored electromagnetic (EM) gap (0.1–10) THz between EM and optical bands; it has piqued the interest of the research community toward 6G because of its favored benefits. THz is regarded as an essential pier for 6G due to its capacity and capabilities to build an

adequate system, supporting a wide range of applications due to its very short wavelength (λ) of 3000–30 μm and other features, e.g., very high frequencies, ultrawide BW, very high data rates, enormous throughput, very low latency, and excellent directivity. THz has encouraged researchers to investigate its capabilities to enable THz communications as it outperforms the two adjacent frequency bands in some ways. THz transmitters/receivers are expected to be manufactured using electronic, photonic, and plasmonic technologies. It is expected to be integrated with optical networks, providing alternate signals for optical pathways in various cases, e.g., backhaul–backhaul, kiosk–node, data center, and intra-device interconnections [13]. As a result, IEEE Std. 802.15.3d–2017 specifies the disadvantages of visible water vapor absorption and path losses, dividing the THz gap across many sub-windows. However, these windows are being thoroughly investigated in order to accommodate 6G services, with certain exceptions in which some 6G services will be incompatible with THz bands [14]. The need for fully connected systems has arisen as a result of Internet of everything (IoE) requirements. There are restrictions to 5G systems that prevent any additions or enhancements to satisfy these needs [15–18].

We aimed to improve wireless connectivity, resource management, scalability, and user fairness, as well as to enhance the overall performance of 6G wireless communications and reliability. Hence, we optimized the current wireless communication systems by utilizing MIMO-NOMA technology and THz frequencies, exploring the performance and gains obtained. The main contributions of this paper are as follows:

(1) We propose a reliable transmission with a non-LOS (NLoS) line of THz communications to overcome THz coverage shortage for open areas or any location where IRS cannot be deployed, in addition to using a simplified cost-effective DF relaying instead of IRS.
(2) We design a system with low power consumption, complexity, and cost by integrating THz, NOMA, MIMO, cooperative networking, and EH (SWIPT) techniques, improving SE, EE, and other metrics compared to the state of the art.
(3) We develop a path-selection mechanism for the potential NOMA-based far users to enhance the system performance and reliability.
(4) Given the flexible structure, we recommend exploiting an existing user in the cell for relaying and not dedicating a fixed device, achieving a synergic coexistence with the expected mobile 6G infrastructure.
(5) To enhance the SIC procedure, we suggest two-user clustering to prevent propagating errors, complications, and spectral deficiencies due to the burden of the additional operations.
(6) We manage the performance and scalability of the spectral and energy efficient upgradeable system, using adjustable parameters and the simplest modulation scheme; hence, this system can be upgraded on the basis of the planner's preferences.

The remainder of this paper is organized as follows: Section 2 gives a brief background of the mechanisms used in this paper; Section 3 describes a number of related studies and the discussed outcomes; Section 4 describes the proposed model and presents the derivation of mathematical closed forms, describing the advantages of the proposed system and the adopted techniques for next generations to achieve the targeted goals; Section 5 describes the system implementation; Section 6 presents the mathematical analysis and simulations, where we model the proposed system by discussing the results and how they bring value to existing systems. The idea behind using the DF relaying user instead of the preceding systems is demonstrated in a discussion centered on enhancing the system performance of THz-NOMA systems, managing the resources; Section 7 summarizes the conclusions of the study.

2. Background

To develop a communication system that meets the extreme values of the emerging requirements in terms of connectivity, SE, latency, data rate, reliability, and user fairness, enabling new applications, EE, and cost-effectiveness, it is necessary to merge some of the

key enabling techniques to achieve the required objectives. As a result, nonorthogonal multiple access in the power domain (NOMA) [19] is the most well-known nominee for developing 6G systems, exceeding the performance of traditional orthogonal multiple access (OMA) schemes. Multiple-input multiple-output (MIMO)-NOMA is the focus of our study. The NOMA mechanism superimposes multiple signals at the transmitter (Tx), and then filters them at the receiver (Rx) by successive interference cancelation (SIC) procedures, thereby increasing channel capacity primarily determined by BW. The interference and noise, on the other hand, are removed by the SIC at the Rx. NOMA multiplexing is achieved by allocating different power coefficients to users on the basis of their channel conditions. At Tx, all users' signals are overlaid. The application of SIC at Rx is used to demultiplex NOMA signals. Because the line of sight (LoS) is the primary transmission path, grouping or clustering of the serviced users is critical for improving SE and reducing the complexity of NOMA-based THz transmission. MIMO-based NOMA BS/users depend basically on channel state information (CSI) (or other metrics often) for successful SIC decoding at the Rx. With a large number of users, user clustering may be difficult; consequently, we strive to design low-complexed systems to solve clustering complications [20,21]. Hence, not only is SIC operation CSI-related, but it can also be quality service-related or hybrid-related [20]. However, all modulation systems have a significant barrier to CSI acquisition at the Tx and Rx [14]. As a result, we employ binary phase-shift keying (BPSK) in the proposed system, which has several advantages over other formats. To address the challenges of THz communications, researchers are looking into all options, highlighting NOMA-assisted cooperative networks. Cooperative networking provides a number of benefits, including increased reliability and capacity, as well as a larger coverage area, all of which improve overall performance, i.e., implementing energy harvesting (EH) with cooperative NOMA [22], which is the focus of the proposed article of THz communications. While applying NOMA to the proposed system, decode-forward (DF) relaying is adopted instead of the complex and costly intelligent reflecting surface (IRS). In NOMA, the far users' signal is already contained in the superposed signal; therefore, that copy can be utilized for relaying. That is preferable to utilizing an additional relaying device with additional complexity and power consumption. While THz-NOMA requires heavy computational SIC operations at the Rx, employing cooperative networking continually drains the relaying user's battery, resulting in system failure. As a result, research activities are aimed at overcoming that issue, transforming into green communications [23] by applying the EH technique. Radiofrequency (RF) power, which exists everywhere surrounding almost all user equipment (UE), is used to send energy and information to distant destinations. Using basic RF circuits, EH allows UEs to harvest that energy. We can then use that gathered power in the broadcasts to convey signals without putting additional strain on the relaying user's battery. Through EH power splitting, the relaying user splits the power it receives into harvesting and decoding fractions, operating them at the same time, resulting in the principle of simultaneous wireless information and power transfer (SWIPT). SWIPT enables the relaying user to capture power from the transmitted signal and use it for data retransmission to a farther user, as depicted in Figure 1. Ultimately, the entire capacity and outage probability (OP) are significantly improved.

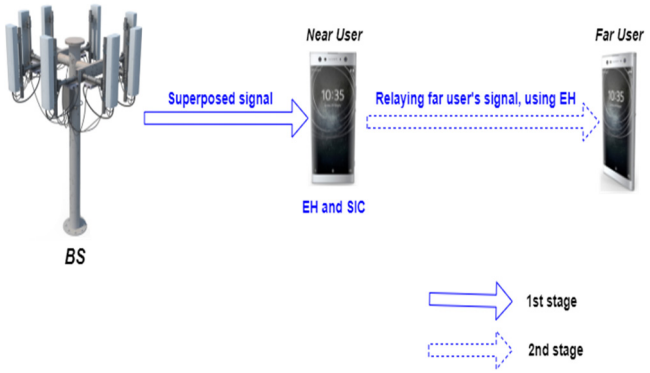

Figure 1. SWIPT with cooperative NOMA.

3. Related Works

Cooperative networking has been previously investigated utilizing a variety of cases and situations; the major benefits were clearly demonstrated while the drawbacks of adopting this strategy were addressed. Other technologies of this study, i.e., EH, NOMA, and THz, were discussed separately or in combination to attain a specific influence on the field. The drawbacks of employing those technologies were thoroughly explored, including the flaws, restrictions, and lack of performance. In [23,24], despite the consideration of the IRS as an edge of technology to improve source to destination transmission in particular cases of interrupted communication path, it must outperform the usage of relaying regarding complexity, energy, and cost, as shown in Figure 2. Briefly, when comparing IRS to the older DF relay, the general impression of this work stated that a supreme data rate is necessary to outperform the DF relay regarding transmit power minimization and EE maximization. Furthermore, IRS requires additional hardware.

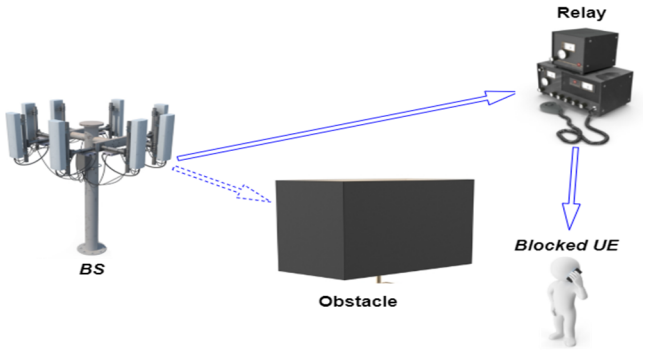

Figure 2. Relay-based transmission strategy.

Tataria et al. [14] discussed the difficulties in designing and deploying IRS to support 6G communication networks, i.e., aligning transmission beams for time-based steering, interference management, and EE degradation. The obstacles that IRS implementation faces include further required procedures, such as the impact of physical coverage area, equipment, system components, and additional maintenance/cost for wireless communications when deploying IRS. Atmospheric effects cause aggregate or proportional failures. IRS uniformity system implementation and interactivity with radio traffic are required for efficient signaling. However, the additional steps will complicate and exhaust network resources. Thus, despite using the promising IRS technology, the proposed system still faces difficulties and noticeable drawbacks.

In [25], clustered, pre-coded, and power-allocated systems were all investigated. They developed an AI-based algorithm to present a clustering technique for THz MIMO-NOMA designs. This methodology comes at the cost of the required running time of the huge dataset, as well as the updated dataset acquisition needed. On the other hand, in [26],

a widely used spatially multiplexed was presented, while sub-THz was investigated to produce very high data rates and spectral efficiency. For data rate maximization, an investigation [27] was conducted for the power allocating issue in NOMA-based cooperative MIMO in HD and FD THz communications, which is still insufficient compared to the assumed targets of the proposed system in this paper.

Oleiwi and Al-Raweshidy studied in their recent work [28] the contribution of EH and other key enabling technologies to enhance system performance, considering a relatively similar concept with a simplified system of single-input single-output (SISO) scheme equipment. However, our previous papers [29,30] investigated the impact of the multihoming principle on improving system reliability, operational efficiency, and the overall performance. The value of multihoming management was addressed to keep communication going for the multihomed user, in addition to presenting an interface selectivity technique.

4. System Model Design

Recent academic and industrial research stated the assumption of deploying ultra-dense heterogeneous networks (UDHNs), with a large number of distributed base stations, access points, relays, and repeaters to the expected 6G densified infrastructure. The presented simple system in Figure 3 is suggested to solve the problems of the THz communications' lack of a coverage area, connection failures, and SIC complexity. Particular use cases are studied, e.g., rural areas, countryside, or any other place where IRS and other supporting equipment cannot be deployed, providing dynamic path selectivity in the case of the user's link failure. The system considers a small cell with MIMO-NOMA-based downlink transmission and two SWIPT-paired clustered users. The BS sends the superimposed signal simultaneously to both NOMA served users, the near user (NU) and the distant user (FU). At a certain moment, the BS to FU path is blocked by an obstruction, resulting in significant shadowing. As a result, the FU is unable to identify its obstructed signal. The NU, on the other hand, establishes a strong connection with the BS. According to NOMA principles, the NU is supposed to first decode the FU's signal before removing it by the SIC process, and then decode its intended signal. Hence, NU receives a copy of the FU's data, such that FU can rely on NU to connect to the BS by exploiting it as a DF relay. For relaying, the energy in the NU's battery is insufficient to convey the data to the FU. To this end, we recommended that NU makes use of EH's power-splitting protocol (SWIPT) to harvest energy from the surrounding RF energy to use it for this retransmission (relaying process). The transmission procedure is divided into two parts. The NU receives the BS superposed signal at the first phase, whereas the power-splitting procedure captures a portion of the NU's harvested power; however, the remaining power is used for data decoding. The captured energy is then used by NU to convey the FU's information to FU in the second phase.

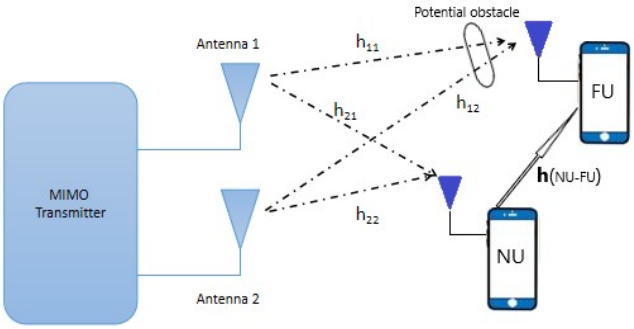

Figure 3. Cooperative SWIPT MIMO-NOMA in THz model.

A Rayleigh fading channel with mean = 0 and variance = Transmission Distance$^{-\text{THz total losses}}$ was conducted in this analysis for all cases. We set additive white gaussian noise (AWGN)

with mean = 0 and variance of σ^2, representing the added noise. The probability density function (PDF) for the point z is given by

$$f_{(z;\sigma)} = \frac{1}{\sqrt{2\pi\sigma^2}} \exp\left(-\frac{z^2}{2\sigma^2}\right). \tag{1}$$

As space attenuation and molecule absorption are considered in the cooperative SWIPT NOMA signal, the path loss of the NLoS link is greater than that of the LoS link. If the LoS link prevails, then the NLoS impact can be ignored [22]. In free space, the THz total loss (η) is set as extraordinarily large. For the users k, the channel gain is written as

$$h_k = \sqrt{A}\sqrt{\frac{1}{\eta}\, G}, \tag{2}$$

where A denotes the MIMO antennas, G denotes the gain of the antenna, and η represents the source–destination THz total losses, written as

$$\eta = \left(\frac{4\pi f d}{C}\right)^2 e^{a(f)d}, \tag{3}$$

where f denotes the THz, d denotes the source–destination distance, $a(f)$ represents the absorbing coefficient, and C denotes the velocity of light.

According to the proposed case, the closed-form derivations are presented below.

Stage 1, BS to NU transmission:

The BS superimposed signal is

$$X = \sqrt{\mathrm{P}}\left(\sqrt{\alpha n}\, xn + \sqrt{\alpha f}\, xf\right), \tag{4}$$

where P denotes the transmit power, αn and αf denote the NU and FU powers, respectively, and xn and xf denote the NU and FU signals, respectively. However, FU cannot detect its signal due to obstruction. The NU signal is given by

$$yn = \sqrt{\mathrm{P}}\left(\sqrt{\alpha n}\, xn + \sqrt{\alpha f}\, xf\right) hsn + wn, \tag{5}$$

$$hsn = (h11 + h12), \tag{6}$$

$$yn = \sqrt{\mathrm{P}}\left(\sqrt{\alpha n}\, xn + \sqrt{\alpha f}\, xf\right)(h11 + h12) + wn, \tag{7}$$

where $hsn\ (h11 + h12)$ is base station to the near user (BS-NU) Rayleigh fading coefficient with mean = 0 and variance of $\mathrm{dsn}^{-\eta}$, dsn denotes the BS-NU distance, and wn is the AWGN with mean = 0 and variance of σ^2. Using yn, NU captures a portion of energy named the EH coefficient (ψ). The remaining energy portion $(1 - \psi)$ is allocated to data decoding. With EH, the data decoded signal is expressed as

$$\begin{aligned} yD &= \left(\sqrt{(1 - \psi)}\right) yn + w\mathrm{eh} \\ &= \left(\sqrt{(1 - \psi)}\right)\sqrt{P}\,\left(\sqrt{\alpha n}\, xn + \sqrt{\alpha f}\, xf\right) + \left(\sqrt{(1 - \psi)}\right) wn \\ &\quad + w\mathrm{eh}, \end{aligned} \tag{8}$$

where $w$eh denotes thermal noise (zero mean and variance of σ^2). For the mathematical process, we abandon the wn harvested energy; consequently, yD is given by

$$\mathrm{yD} = \left(\sqrt{(1 - \psi)}\right)\sqrt{P}\,\left(\sqrt{\alpha n}\, xn + \sqrt{\alpha f}\, xf\right) + w\mathrm{eh}. \tag{9}$$

As a function of yD, NU decodes xf straightaway. The NU rate to decode FU's data is calculated as

$$Rnf = \frac{1}{2}\log_2\left(1 + \frac{(1-\psi)\mathrm{P}\ \alpha\mathrm{f}\ |h11 + h12|^2}{(1-\psi)\mathrm{P}\ \alpha n|h11 + h12|^2 + \sigma^2}\right). \tag{10}$$

With SIC, the NU rate of NU information decoding is calculated as

$$Rnf = \frac{1}{2}\log_2\left(1 + \frac{(1-\psi)\mathrm{P}\ \alpha n\ |h11 + h12|^2}{\sigma^2}\right), \tag{11}$$

where ψ is the captured EH coefficient during the first phase. EH is calculated as

$$PH = P\ |h11 + h12|^2\ \zeta\ \psi, \tag{12}$$

where ζ denotes the circuitry EH efficiency.

Stage 2, NU to FU DF-relaying:

Using the gathered energy, NU conveys the data to FU (PH). As a result, the NU's sent signal is

$$\sqrt{\mathrm{PH}}\,\widetilde{xf}. \tag{13}$$

The detected signal at FU is given by

$$\sqrt{\mathrm{PH}}\,\widetilde{xf}hnf + wf, \tag{14}$$

$$hf = min\{(h21 + h22),\ hnf\}, \tag{15}$$

where hf denotes the minimal Rayleigh fading channel of the selected path between the BS and FU (i.e., $(h21 + h22)\ or\ hnf$), and hnf is the NU-to-FU Rayleigh channel. The rate of the FU is represented as

$$Rf = \frac{1}{2}\log_2\left(1 + \frac{PH|hf|^2}{\sigma^2}\right). \tag{16}$$

In the first stage, NU is supposed to decode the FU's information in order to determine the ideal power-splitting coefficient, allowing it to properly retransmit FU's data. To do so, the constraint $Rnf > Rf*$ was set.

The FU target rate is $Rf*$. This criterion implies that the NU rate for decoding FU data must be higher than the FU intended rate. To derive ψ, Rnf in Equation (11) is substituted into the assumed constraint presented above.

$$\frac{1}{2}\log_2\left(1 + \frac{(1-\psi)\mathrm{P}\ \alpha\mathrm{f}\ |hf|^2}{(1-\psi)\mathrm{P}\ \alpha n|hf|^2 + \sigma^2}\right) > Rf*. \tag{17}$$

$$\log_2\left(1 + \frac{(1-\psi)\mathrm{P}\ \alpha\mathrm{f}\ |hf|^2}{(1-\psi)\mathrm{P}\ \alpha n|hf|^2 + \sigma^2}\right) > 2Rf*. \tag{18}$$

$$\frac{(1-\psi)\mathrm{P}\ \alpha\mathrm{f}\ |hf|^2}{(1-\psi)\mathrm{P}\ \alpha n|hf|^2 + \sigma^2} > 2^{2Rf*} - 1. \tag{19}$$

The term $2^{2\mathrm{Rf}*} - 1$ is represented by τf to denote the FU targeted SINR.

$$\frac{(1-\psi)\mathrm{P}\ \alpha\mathrm{f}\ |hf|^2}{(1-\psi)\mathrm{P}\ \alpha n|hf|^2 + \sigma^2} > \tau f. \tag{20}$$

$$(1-\psi)P\ \alpha f\ |hf|^2 > \tau f(1-\psi)\mathrm{P}\ \alpha n|hf|^2 + \tau\mathrm{f}\sigma^2. \tag{21}$$

$$(1-\psi)P\ \alpha f\ |hf|^2 - \tau f(1-\psi)\mathrm{P}\ \alpha n|hf|^2 > \tau\mathrm{f}\sigma^2. \tag{22}$$

$$(1-\psi)P\left|hf\right|^2\left(\alpha f-\tau f\alpha n\right)>\tau f\sigma^2. \tag{23}$$

$$\psi\ <\ 1-\frac{\tau f\sigma^2}{\mathrm{P}\left|hf\right|^2\left(\alpha f-\tau f\alpha n\right)}. \tag{24}$$

To guarantee a smaller value of ψ, the above equation can be reshaped as

$$\psi\ =1-\frac{\tau f\sigma^2}{\mathrm{P}\left|hf\right|^2\left(\alpha f-\tau f\alpha n\right)}-\delta, \tag{25}$$

where δ is represented by a very small value (i.e., 10^{-6}); then, ψ guarantees the needed energy to decode the data, achieving the FU targeted rate.

Outage Probability:

It is every user's chance that the data rate will drop beneath the target. $Rn*$ and $Rf*$ (bits/s/Hz) are the NU and FU targeted rates, respectively.

FU is considered to fail whenever Rf in Equation (16) is smaller than targeted rate, represented as

$$\mathrm{PNU}=\Pr(Rf\ <\ Rf*). \tag{26}$$

The NU must accurately decode both signals: the FU signal and its signal. The NU and FU targeted rates must be equal to the NU rate. When using SIC, if the NU or FU targeted rates in Equations (11) and (16) are not sufficient, NU experiences an outage, which is represented by

$$\mathrm{PNU}=\Pr(\mathrm{RNF}\ <\ Rf*)\ +\ \Pr(\mathrm{RNF}\ >\ Rf*,\ Rn<\ Rn*). \tag{27}$$

We follow up on the first mode described in the PHY section of [31] of the THz single carrier frequency. This idea is recommended for high-speed transmission links aimed at bandwidth-based cases, e.g., links of backhaul/backhaul, fronthaul/backhaul, and between data center racks [32]. Due to atmosphere and impact, the accessible spectrum is divided into multiple channels on the basis of the spectral windows of THz frequencies (from 252.72 to 321.84) GHz, with each channel having its own features [32]. There are multiple cases of 2.16 GHz within the THz spectrum, whereby six channels and eight bands (from 2.16 to 69 GHz) are discovered. According to some criteria and constraints, these spectral windows can be determined.

Despite the variety of available modulation types in THz-SC PHY (BPSK and QPSK are required), we utilize BPSK as the simplest scheme among the different supported modulations. Transmission distance and system performance are the critical measures that must be balanced on the basis of system metrics, considering a range-to-rate tradeoff strategy [28].

5. Implementation

The first implementation is to show that our simulation is valid when compared to the mathematical analysis. The simulation described below compares the recent similar system equipped with the SISO scheme as a baseline to this paper's scenario of cooperative SWIPT THz MIMO-NOMA, utilizing moderated parameter settings for transmit frequency, allocated BW, transmit power, and transmit distance.

(1) Transmit power, frequency, distance, and BW can be adjusted.
(2) Targeted rates are 1 Gbps for the FU and 3 Gbps for the NU.
(3) A power of −30 to 30 dBm is dedicated to cover a wider area if the FU goes farther. Hence, transmit power can be reduced.
(4) We set a relatively high path-loss exponent η = 4; hence, it can be reduced. The absorption coefficient can be found in [27]. The simulations were implemented using MATLAB$^{(r)}$.

6. Simulation Results

This section includes the implementation of simulations and numerical analysis to verify the validation of data rates and OP. The simulation findings confirm the obtained closed forms of the optimized model, and they are compared to earlier research. By existing an obstruction in the link to the BS, the presented mechanism should allow the obstructed user to maintain continuous communication. The sections below explain how the proposed system and mechanism can enhance EE, SE, reliability, and system performance by addressing the distance-limited communications of THz frequencies. Table 1 shows the simulation parameters.

Table 1. Simulation parameters.

Notation	Parameters	Value
f	Frequency	311.04 GHz
BW	Bandwidth	12.96 GHz
P	Transmission power	30 dBm
d	Transmission distance	Phase 1 = 20 m Phase 2 = 30 m
αn	NU power coefficient	0.25 of total power
αf	FU power coefficient	0.75 of total power
G	Antenna gain	25 dB
eta	Path loss exponent	4
	Target data rate	3, 1 Gbps for NU, FU

6.1. System Validity Analysis

In contrast, a mathematical analysis and simulation were carried out to compare the system sum throughput and OP, using a transmission power of 20 dBm for system validation, verifying the intended objectives.

Figures 4 and 5 exhibit the striking match between the mathematical analysis of the derived close forms and simulation results. They confirm the analysis accuracy and system validity, now including the uniqueness of new values. We thoroughly study system metrics throughout the remaining parts of this paper.

Sum Throughput Versus Transmit Power:

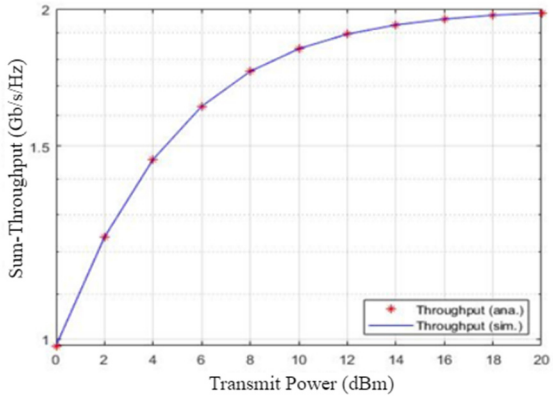

Figure 4. Throughput vs. transmit power.

Users' OP versus Transmit Power:

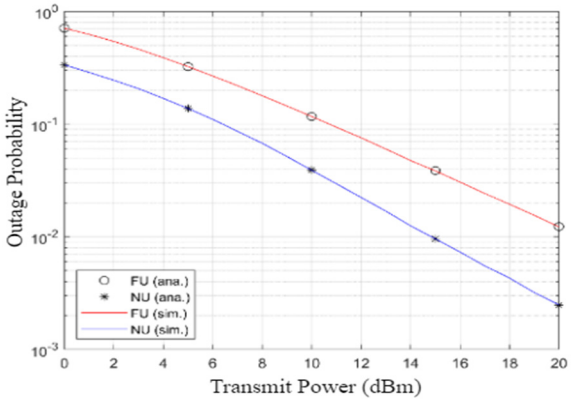

Figure 5. OP vs. Transmit Power.

6.2. System Simulation

First, the performance of the system's served users was individually implemented, and then we examined the entire system's sum rate. The performance was compared with our previous similar SISO-based system model (as a baseline) to explain how the presented system provides a remarkable improvement of the current wireless communication systems, by employing the edge of technologies mentioned in this paper.

6.2.1. Achievable Users' Rates versus Transmit Power

Figure 6 demonstrates the system users' performance versus the dedicated power. For the two users, the MIMO technique provides remarkable leverage to system performance compared to the SISO scheme. The NU performs much better than the FU, despite the EH technique allocating the essential energy to achieve the target rate and harvesting the remainder for retransmission, thus clarifying the impact of comparative THz losses. However, the FU still achieves a data rate greater than the target despite the interference it experiences (as the FU does not perform the SIC process). Furthermore, we can make use of the harvested power for further EH processes.

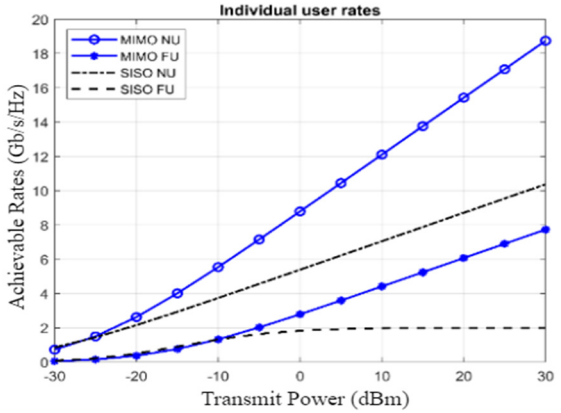

Figure 6. Rates vs. transmit power.

6.2.2. OP versus Transmit Power

Similarly, for both NOMA users, the MIMO technique provides a notable enhancement of system performance compared to the SISO scheme, as shown in Figure 7. In spite of having more dedicated power than the NU, the FU has a higher outage. This reflects the expected performance given their distinct channel variations.

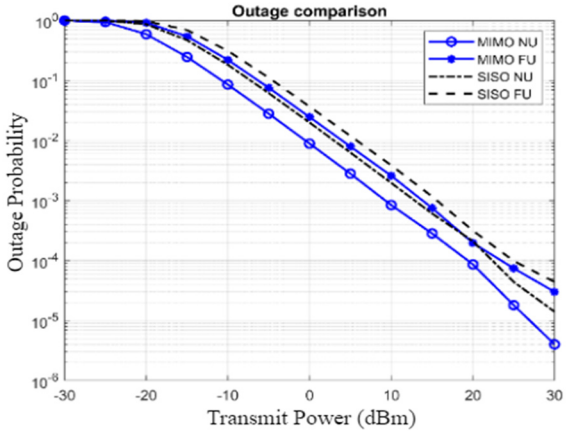

Figure 7. OP vs. transmit power.

6.2.3. Achievable Sum Rates versus Transmit Power

In Figure 8, it is proven that the MIMO technique provides added value through a remarkable impact on the system performance compared to the SISO scheme. Moreover, the presented system outperforms the state of the art considering our simpler and cost-effective model, which has lower complexity and achieves higher EE and SE. Hence, we achieve the same target for the two users using relatively less power than allocated in previous research (e.g., [27]). This demonstrates the significance of using the energy-harvesting technique with the proposed strategy, representing additional gain and a significant contribution.

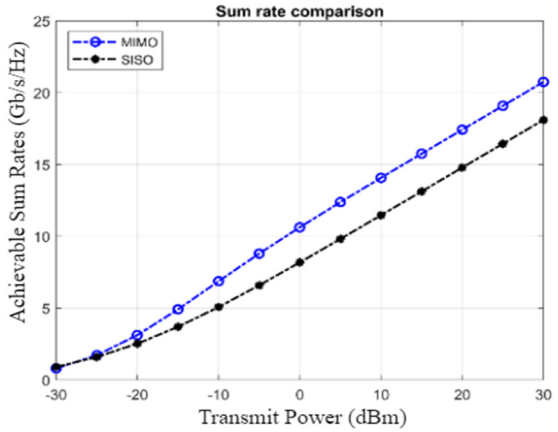

Figure 8. Sum rates vs. transmit power.

In contrast, MIMO-NOMA systems might face some drawbacks, e.g., the computational complications of MIMO and procedural complexity of SIC-dependent NOMA, as SIC is widely thought to be implemented flawlessly, notwithstanding the possibility of procedural errors. Thus, it is critical to keep the number of users per cluster as low as possible, as user CSI acquisition has a significant impact on SIC implementation.

7. Conclusions

This paper thoroughly studied the application of the EH technique to a cooperative MIMO-NOMA system for THz communications. The EH coefficient was derived to verify the intended SINR, data rates, and spectral efficiency for MIMO-NOMA served users. The maximal possible comparable EH-based energy efficiency was examined in accordance with a 1 Gbps reference point to the far user and 3 Gbps to the near user. The system outperformed comparable studies (e.g., similar cooperative MIMO-NOMA THz communication system) in terms of gain with a simpler design. Furthermore, it outperformed our previous work using a similar simplified system with an SISO scheme, providing better

overall performance (in terms of reliability, OP, SE, and EE) by more than 50% (with a doubled individual user gain), considering the simplicity and reliability tradeoff. Overall, the findings demonstrated how the defined strategies successfully preserved continued communication between the BS and the potentially obstructed FU, as well as how the overall system performance was greatly enhanced. Additionally, this work provided a dynamic path-selection mechanism for further reliability. Moreover, it is worth noticing that the scalability of the system presents a flexible adaptation for system planners as the examined parameters are adjustable according to the deployment situations. To the best of the authors' knowledge, SWIPT has never been adopted with such a system of cooperative THz MIMO-NOMA systems achieving such results. The SE, EE, and reliability have not previously been improved, especially using the dynamic mechanism we adopted.

Author Contributions: Conceptualization, H.W.O.; methodology, H.W.O.; software, H.W.O.; validation, H.W.O.; formal analysis, H.W.O.; investigation, H.W.O.; resources, H.W.O.; data curation, H.W.O.; writing—original draft preparation, H.W.O.; writing—review and editing, N.S.; visualization, N.S.; supervision, H.A.-R.; project administration, H.A.-R.; funding acquisition, N.S. All authors have read and agreed to the published version of the manuscript.

Funding: This research received no external funding.

Conflicts of Interest: The authors declare no conflict of interest.

References

1. Han, S.; Xie, T.; Chih-Lin, I. Greener Physical Layer Technologies for 6G Mobile Communications. *IEEE Commun. Mag.* **2021**, *59*, 68–74. [CrossRef]
2. Jiang, W.; Han, B.; Habibi, M.A.; Schotten, H.D. The Road Towards 6G: A Comprehensive Survey. *IEEE Open J. Commun. Soc.* **2021**, *2*, 334–366. [CrossRef]
3. Alsabah, M.; Naser, M.A.; Mahmmod, B.M.; Abdulhussain, S.H.; Eissa, M.R.; Al-Baidhani, A.; Noordin, N.K.; Sait, S.M.; Al-Utaibi, K.A.; Hashim, F. 6G Wireless Communications Networks: A Comprehensive Survey. *IEEE Access* **2021**, *9*, 148191–148243. [CrossRef]
4. Alwis, C.; De Kalla, A.; Pham, Q.V.; Kumar, P.; Dev, K.; Hwang, W.J.; Liyanage, M. Survey on 6G Frontiers: Trends, Applications, Requirements, Technologies and Future Research. *IEEE Open J. Commun. Soc.* **2021**, *2*, 836–886. [CrossRef]
5. Rappaport, T.S.; Xing, Y.; Kanhere, O.; Ju, S.; Madanayake, A.; Mandal, S.; Alkhateeb, A.; Trichopoulos, G.C. Wireless Communications and Applications Above 100 GHz: Opportunities and Challenges for 6G and Beyond. *IEEE Access* **2019**, *7*, 78729–78757. [CrossRef]
6. Liu, Y.; Liu, F.; Zhu, G.; Wang, X.; Jiao, Y. Dynamic Power Optimization of Pilot and Data for Downlink OFDMA Systems. *J. Commun. Netw.* **2021**, *23*, 250–259. [CrossRef]
7. Chatzimisios, P.; Soldani, D.; Jamalipour, A.; Manzalini, A.; Das, S.K. Special Issue on 6G Wireless Systems. *J. Commun. Netw.* **2020**, *22*, 440–443. [CrossRef]
8. Darsena, D.; Gelli, G.; Verde, F. Design and Performance Analysis of Multiple-relay Cooperative MIMO Networks. *J. Commun. Netw.* **2019**, *21*, 25–32. [CrossRef]
9. Sun, Y.; Cyr, B. Sampling for Data Freshness Optimization: Non-linear Age Functions. *J. Commun. Netw.* **2019**, *21*, 204–219. [CrossRef]
10. Akyildiz, I.F.; Kak, A.; Nie, S. 6G and Beyond: The Future of Wireless Communications Systems. *IEEE Access* **2020**, *8*, 133995–134030. [CrossRef]
11. Gür, G. Expansive Networks: Exploiting Spectrum Sharing for Capacity Boost and 6G Vision. *J. Commun. Netw.* **2020**, *22*, 444–454. [CrossRef]
12. Elayan, H.; Amin, O.; Shihada, B.; Shubair, R.M.; Alouini, M.S. Terahertz Band: The Last Piece of RF Spectrum Puzzle for Communication Systems. *IEEE Open J. Commun. Soc.* **2020**, *1*, 1–32. [CrossRef]
13. Sarieddeen, H.; Alouini, M.S.; Al-Naffouri, T.Y. An Overview of Signal Processing Techniques for Terahertz Communications. *Proc. IEEE* **2021**, *109*, 1628–1665. [CrossRef]
14. Tataria, H.; Shafi, M.; Molisch, A.F.; Dohler, M.; Sjoland, H.; Tufvesson, F. 6G Wireless Systems: Vision, Requirements, Challenges, Insights, and Opportunities. *Proc. IEEE* **2021**, *109*, 1166–1199. [CrossRef]
15. Fan, D.; Gao, F.; Wang, G.; Zhong, Z.; Nallanathan, A. Channel Estimation and Transmission Strategy for Hybrid mmWave NOMA Systems. *IEEE J. Sel. Top Signal Process* **2019**, *13*, 584–596. [CrossRef]
16. Wang, C.; Qin, C.; Yao, Y.; Li, Y.; Wang, W. Low Complexity Interference Alignment for mmWave MIMO Channels in Three-Cell Mobile Network. *IEEE J. Sel. Areas Commun.* **2017**, *35*, 1513–1523. [CrossRef]
17. Liang, W.; Ding, Z.; Li, Y.; Song, L. User Pairing for Downlink Non-Orthogonal Multiple Access Networks Using Matching Algorithm. *IEEE Trans. Commun.* **2017**, *65*, 5319–5332. [CrossRef]

18. Zhong, D.; Deng, D.; Wang, C.; Wang, W. Maximizing Downlink Non-Orthogonal Multiple Access System Capacity by A Hybrid User Pairing Strategy. In Proceedings of the 2021 IEEE/CIC International Conference on Communications in China (ICCC), Xiamen, China, 28–30 July 2021; pp. 712–717. [CrossRef]
19. Krishnamoorthy, A.; Schober, R. Uplink and Downlink MIMO-NOMA with Simultaneous Triangularization. *IEEE Trans. Wirel. Commun.* **2021**, *20*, 3381–3396. [CrossRef]
20. Liu, Y.; Zhang, S.; Mu, X.; Ding, Z.; Schober, R.; Al-Dhahir, N.; Ekram, H.; Xuemin, S. Evolution of NOMA Toward Next Generation Multiple Access (NGMA) for 6G. *IEEE J. Sel. Areas Commun.* **2022**, *40*, 1037–1071. [CrossRef]
21. Maraqa, O.; Rajasekaran, A.S.; Al-Ahmadi, S.; Yanikomeroglu, H.; Sait, S.M. A Survey of Rate-Optimal Power Domain NOMA with Enabling Technologies of Future Wireless Networks. *IEEE Commun. Surv. Tutor.* **2020**, *22*, 2192–2235. [CrossRef]
22. Liaqat, M.; Noordin, K.A.; Abdul Latef, T.; Dimyati, K. Power-domain Non Orthogonal Multiple Access (PD-NOMA) in Cooperative Networks: An Overview. *Wirel Netw.* **2020**, *26*, 181–203. [CrossRef]
23. Ng, D.W.K.; Duong, T.Q.; Zhong, C.; Schober, R. *Wireless Information and Power Transfer: Theory and Practice*; Wiley Press: Hoboken, NJ, USA, 2018; ISBN 9781119476863.
24. Bjornson, E.; Ozdogan, O.; Larsson, E.G. Intelligent Reflecting Surface Versus Decode-and-Forward: How Large Surfaces are Needed to Beat Relaying? *IEEE Wirel. Commun. Lett.* **2020**, *9*, 244–248. [CrossRef]
25. Zhang, H.; Zhang, H.; Liu, W.; Long, K.; Dong, J.; Leung, V.C.M. Energy Efficient User Clustering, Hybrid Precoding and Power Optimization in Terahertz MIMO-NOMA Systems. *IEEE J. Sel. Areas Commun.* **2020**, *38*, 2074–2085. [CrossRef]
26. Saad, M.; Al Akkad, N.; Hijazi, H.; Al Ghouwayel, A.C.; Bader, F.; Palicot, J. Novel MIMO Technique for Wireless Terabits Systems in Sub-THz Band. *IEEE Open J. Veh. Technol.* **2021**, *2*, 125–139. [CrossRef]
27. Elkharbotly, O.; Maher, E.; El-Mahdy, A.; Dressler, F. Optimal Power Allocation in Cooperative MIMO-NOMA with FD/HD Relaying in THz Communications. In Proceedings of the 2020 9th IFIP International Conference on Performance Evaluation and Modeling in Wireless Networks, PEMWN 2020, Berlin, Germany, 1–3 December 2020.
28. Oleiwi, H.W.; Al-Raweshidy, H. Cooperative SWIPT THz-NOMA / 6G Performance Analysis. *Electronics* **2022**, *11*, 873. [CrossRef]
29. Oleiwi, H.W.; Mhawi, D.N.; Saeed, N. A Comparative Investigation on Different QoS Mechanisms in Multi-homed Networks. *Iraqi J. Ind. Res.* **2022**, *9*, 1–10. [CrossRef]
30. Oleiwi, H.W.; Saeed, N.; Mhawi, D.N. An Enhanced Interface Selectivity Technique to Improve the QoS for the Multi-homed Node. *Eng. Technol. J.* 2022, in press.
31. *IEEE 802.15.3d-2017*; IEEE Standard for High Data Rate Wireless Multi-Media Networks—Amendment 2: 100 Gb/s Wireless Switched Point-to-Point Physical Layer. IEEE: Manhattan, NY, USA, 2017; Volume 2017, ISBN 9781504442466.
32. Petrov, V.; Kurner, T.; Hosako, I. IEEE 802.15.3d: First Standardization Efforts for Sub-Terahertz Band Communications Toward 6G. *IEEE Commun. Mag.* **2020**, *58*, 28–33. [CrossRef]